Advances in Research

22(2): 1-11, 2021; Article no.AIR.66992
ISSN: 2348-0394, NLM ID: 101666096

Sugar Transport in a Merging Phloem Vessels: A Hydrodynamic Model

W. I. A. Okuyade[1], T. M. Abbey[2] and M. E. Abbey[1*]

[1]School of Applied Sciences, Federal Polytechnic of Oil and Gas, Bonny Island, Nigeria.
[2]Department of Physics, Applied Mathematics and Theoretical Physics Group, University of Port Harcourt, Port Harcourt, Nigeria.

Authors' contributions

This work was carried out in collaboration among all authors. All authors whose names appear on this article made substantial contributions in the following ways: Conception or design of the work, analysis and interpretation of data. All authors read and approved the final manuscript.

Article Information

DOI: 10.9734/AIR/2021/v22i230293
Editor(s):
(1) Dr. Martin Kröger, Swiss Federal Institute of Technology (ETH Zürich), Switzerland.
Reviewers:
(1) Elisa Gatto, University of Salento, Italy.
(2) Nuryazmeen Farhan binti Haron, University Teknologi MARA Shah Alam Selangor, Malaysia.
Complete Peer review History: http://www.sdiarticle4.com/review-history/66992

Original Research Article

Received 02 February 2021
Accepted 07 April 2021
Published 16 April 2021

ABSTRACT

Green plants are the major tappers of the energy from the sun. The collected solar energy in the form of light is used to activate the chemical reaction occurring in matured leaves between carbon dioxide and water, leading to the synthesis of sugar (chemical energy). Two main transport processes are involved in the transport of mineral salt water from the soil through the roots, via the trunk and branches to the leaves where photosynthetic activity occurs, and the translocation of sugar from the leaves to where they are needed and possibly, stored. The xylem vessels bear the absorbed mineral salt water while the phloem vessels bear the manufactured sugar. In this study, neglecting the effects of occlusion and clogging of the phloem channels, we investigate the transport of sugars in the merging phloem vessels using the hydrodynamic approach. The model is designed using the Boussinesq approximation and solved semi-analytically using the regular perturbation series expansion solutions and Mathematica 11.2 computational software. Expressions for the concentration, temperature, and velocity are obtained and presented quantitatively and graphically. The results show among others, that increase in the merging angle causes a reduction in the concentration, temperature, and velocity profiles. However, there exists fluctuations in the concentration and temperature structures.

**Corresponding author: E-mail: abbeyminaibim@gmail.com;*

Keywords: merging flow; bifurcating flow; green plants; phloem flow; xylem flow.

1. INTRODUCTION

Merging flows have applications in external flows such as lakes, rivers, and estuaries; internal flows such as internal machinery, respiratory system, materials transport in bifurcating green plants, transport of oxygenated and deoxygenated blood in mammals, etc.

Plant hair roots absorb mineral salt water, which is at lower osmotic pressure from the soil into the vacuoles which are at higher osmotic pressure, and conduct it radially into the xylem vessels of the roots, from where it is carried through the trunk and branches to the leaves. A continuous water column that connects the leaves to the soil water is created through the high capillary force that is developed in the leaves' cell walls. As the leaves are in a very dry atmosphere, much of the water at the top of the water column evaporates into the atmosphere through the opening of the stomata. The loss of water in the column causes the capillary force to exert strong pull/suction pressure on it. The pull causes the sap to ascend the plant, thereby creating room for more water to be absorbed by the roots at the other end. Thus, the higher the evaporation in the leaves, the higher the tension and absorption rate in the roots [1]. The continuous absorption of water into the plant is believed to be influenced by two forces: root pressure and suction pressure. The root pressure is the pressure at the roots by which the soil water is drawn into the root hairs. It is known to be active at night when humidity is high and the temperature is low. The suction pressure is the pressure in a cell by which the fluid in a neighboring cell is drawn into it. It is set up during the day in the presence of sunlight. The xylem vessels are under negative pressure of magnitude -2MPa [2]. Furthermore, at the opening of the stomata, some water evaporates into the atmosphere and carbon dioxide diffuses into the leaves. The carbon dioxide reacts with a bit of the water in the mesophyll cells of the matured leaves in the presence of sunlight as the activation energy to form sugars (species) through photosynthesis. The sugar (assimilate) is translocated to the new leaves, shoots, fruits, roots, etc. where they are needed for metabolism and growth or stored [1-3]. Therefore, the sugars provide the building materials for the growth of the plant. The sugars are transported to other parts of the plant through the phloem vessels.

Evidently, the vascular green plant is made up of two main conducting components: the xylem and phloem. These play very important roles in the plants' life. The xylem, which is protected inside the plant, comprises the tracheid and large thick-walled tubes or vessels. They are segmented and porous; they do not contain cytoplasm, and as such are said to be dead vessels. They carry the mineral salt water (solution) absorbed from the soil through the roots via the trunk and branches to the leaves. On the other hand, the phloem vessels are found inside the bark of plants. They consist of living cylindrical sieve tubes or elements perforated cross walls and arranged end-to-end in long rows. As living cells, they contain cytoplasm, nuclei, and saps, which are at high osmotic pressure. They carry synthesized carbohydrates (produced in the matured leaves), protein, fat and oil, hormones, etc. (all produced in the leave epical meristem of young growing shoots, developing seeds and fruits) to where they are needed or stored.

Some interactions exist between the xylem and phloem vessels along the entire length of the plant in the process of fluid exchange. The interaction is strong in the leaves at the outlets of the xylem (tracheary elements) and the inlet of the phloem (sieve elements) separated by a few microns [2]. Part of the water coming out of the tracheary elements of the mesophyll cells ends up in the nearby sieve elements, and this helps in pushing the sugars through the phloem vessels. The transport mechanism in the phloem is driven by the differences in the osmotic pressure (Munch mechanism) which is caused by the differences in the concentration between the source and sink of the sugars [2]. More so, it is affected by some hydrodynamic, physical, and environmental parameters. It is noteworthy that, sometimes the flow in the phloem vessels is disturbed by the occlusion of the channel due to forisomes (contractile protein) or the clogging of the sieve plates [3].

There are a limited number of reports on merging flows in plants and animal circulatory processes. This implies that the phenomenon has not been well worked on by researchers. Among the few existing pieces of literature, both symmetric and asymmetric cases were considered using the Newtonian fluid principle. For example, [4] considered blood flow through a straight channel with an upstream splitter plate; [5], neglecting the effects of pulsatility, investigated a two-dimensional merging blood flow in a basilar artery using geometrical transformation, conformal mapping and numerical approaches; [6] numerically examined a steady two-dimensional asymmetric merging flow of a micro-polar fluid in a rectangular channel.

More so, there are reports on vascular plant biology and its bio-mechanics. These include introductory books, literature overviews, and bio-mechanical models. Among the introductory books are [7-11]. Among the literature overviews are [2,12-16], etc. Specifically, [2] is a follow-up of [12] and [16], which reviewed the physical mechanics involved in sap transport in the xylem vessels. They overviewed the flow in the phloem vessels using the fluid dynamic approach. Amidst the biomechanical models of green plants, we have [17], who worked on the xylem and phloem flows in a tree trunk using the method of Laplace transforms; [18-20] studied the normal and oscillatory xylem flow in bifurcating green plants using the method of perturbation series expansions, and observed that for the normal flow while the increase in the heat exchange parameter increases the temperature, increase in the bifurcation angle increases the velocity and concentration. For the oscillatory flow, they noticed the increase in the bifurcation angle increases the velocity but decreases the concentration; the increase in a magnetic field, chemical reaction rate, heat exchange, buoyancy parameters, Peclet number, and Reynolds number increase the concentration and velocity factors.

In particular, the energy budget of plants with the resources (water, nutrients, carbon dioxide, and light) are extremely important for their metabolism, growth, and reproduction. Naturally, some of these resources needed for the plants' welfare may be present but may not get to the zones where they are needed promptly due to some physiologic, physical, chemical, and environmental factors. Down-playing the physio-geometric factors such as the effects of occlusion and clogging of the sieve tubes, in this paper, we investigate hydro-dynamically the translocation of sugars from the matured leaves via the branches through the trunk to the roots.

2. MATHEMATICAL FORMULATION AND PHYSICS OF THE PROBLEM

We consider the merging flow of synthesized sugar solution in a bifurcating green plant. The physical model is shown in Fig.1. The fluid is moving downward through the merging channels. Therefore, the axial velocity is in the direction of gravity. We assume the flow is osmotically driven and free convective since the plant has no pumps; the Reynolds number of the flow is less than unity, therefore, the inertia terms are zero and the flow a slow one; there is an existing interaction between the plant and its environment such that the effects of heat exchange and radiation from the sun are significant; the channels are porous, cylindrical, and axisymmetric; the fluid (synthesized sugar solution) is viscous, incompressible, Newtonian; the chemical reaction occurring in the leaves during photosynthesis leads to the production of sugar species is of order one; the flow velocity in the θ-axis is symmetric so that the variation about it is zero, and for a two-dimensional flow, the velocity components are (u', w') in the (r', z') orthogonal coordinates. Similarly, since the manufactured sugars in the plant are under the same condition of temperature and concentration, and the channels are symmetrical, then only a set of equations satisfies the problem. Upon these, considering the Boussinesq approximation, the equations of mass balance, momentum, energy, and diffusion are.

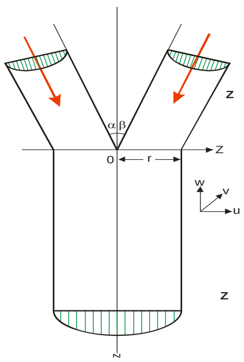

Fig. 1. A Schematic of a Bifurcating Green Plant

$$\frac{1}{r}\frac{\partial}{\partial r}(r'u') + \frac{\partial w'}{\partial r'} = 0 \quad (1)$$

$$0 = -\frac{\partial p'}{\partial r'} + \mu\left(\frac{\partial^2 u'}{\partial r'^2} + \frac{1}{r'}\frac{\partial u'}{\partial r'} + \frac{u'}{r'^2} + \frac{\partial^2 u'}{\partial z'^2}\right) \quad (2)$$

$$0 = -\frac{\partial p'}{\partial z'} + \mu\left(\frac{\partial^2 w'}{\partial r'^2} + \frac{1}{r'}\frac{\partial w'}{\partial r'} + \frac{\partial^2 w'}{\partial z'^2}\right) - \rho g \beta_1 (T' - T_\infty) - \rho g \beta_2 (C' - C_\infty) - \frac{\mu}{\kappa} w' \quad (3)$$

$$u'\frac{\partial T'}{\partial r'} + w'\frac{\partial T'}{\partial z'} = -\frac{k}{\rho C_p}\left(\frac{\partial^2 T'}{\partial r'^2} + \frac{1}{r'}\frac{\partial T'}{\partial r'} + \frac{\partial^2 T'}{\partial z'^2}\right) + \frac{Q(T' - T_\infty)}{\rho C_p} \quad (4)$$

$$u'\frac{\partial C'}{\partial r'} + w'\frac{\partial C'}{\partial z'} = D\left(\frac{\partial^2 C'}{\partial r'^2} + \frac{1}{r'}\frac{\partial C'}{\partial r'} + \frac{\partial^2 C'}{\partial z'^2}\right) + k_r^2(C' - C_\infty) \quad (5)$$

where p' is the fluid pressure, μ is the fluid viscosity, ρ is the fluid density, g is the gravitational field vector, T' and C' are the fluid temperature and concentration, k is the fluid thermal conductivity, C_p is the fluid specific heat capacity at constant pressure, k_r^2 is the chemical reaction rate, T_w and C_w are the constant temperature and concentration at the wall, T_∞ and C_∞ are the fluid equilibrium temperature and concentration, β_1 and β_2 are the volumetric expansion coefficients for temperature and concentration of the fluid, κ is the permeability of the porous medium, Q is the fluid heat absorption/generation coefficient, D is the fluid diffusion coefficient.

Fig.1 shows that the channel is symmetrical and split into two regions: the upstream $z < Z$ and downstream $z > Z$, where z is the nodal or merging point taken as the origin, such that the boundaries become $r' = \alpha z'$ for the upstream and $r' = \pm 1$ the downstream. Because of the geometrical transition between the upstream and downstream regions of the channel the issue of wall curvature arises. Effecting this, a simple transition wherein the diameter of the upstream region is made equal to half that of the downstream region is assumed such that the variation of the angle of merging is used straight-forwardly [20]. Additionally, the diameter of the downstream is assumed to be far less than the length such that $\frac{d}{l} = \psi << 1$ such that the flow is laminar and Poiseuille [17,21]; [17,21]. Based on the above, the boundary conditions become:

for the upstream region, $z < Z$

$$u' = 0, w' = 0, T' = 0, C' = 0 \text{at} r' = 0 \quad (6)$$

$$u' = 0, w' = 0, T' = \xi_1 T_w, C' = \xi_2 C_w, \xi_{1,} = \xi_2 < 1 \text{ at } r' = \alpha z' \quad (7)$$

and for the downstream region, $z > Z$

$$u' = 1, w' = 1, T' = T_\infty, C' = C_\infty \text{at } r' = 0 \quad (8)$$

$$u' = 0, w' = 0, T' = T_w, C' = C_w \text{ at } r' = 1 \quad (9)$$

Introducing the following dimensionless quantities:

$$z = \frac{\psi z'}{l}, r = \frac{r'}{R_o}, \Theta = \frac{T' - T_\infty}{T_w - T_\infty}, \Phi = \frac{C' - C_\infty}{C_w - C_\infty}, w = \frac{w' r_o}{l}, p = \frac{(p' - p_\infty) r_o^3}{\rho l v}, \quad n^2 = \frac{Q}{k},$$

$$\chi^2 = \frac{r_o}{\kappa}, \delta_1^2 = \frac{k_r^2}{D}, Sc = \frac{v}{D}, Pr = \frac{\mu Cp}{k_o}, Gr = \frac{g\beta_1 (T_w - T_\infty)}{v^2}, Gc = \frac{g\beta_2 (C_w - C_\infty)}{v^2} \quad Re = vl, Pe_m = Re\,S\,c, Pe_h = RePr$$

where Θ and Φ are the non-dimensionalized temperature and concentration; v is the kinematic viscosity; l is the characteristic length of the tube; r_o is the characteristic radius of the capillary; Re is the Reynolds number; n^2 is the environmental temperature differential parameter, otherwise called the Heat exchange parameter; χ^2 is the porosity parameter; δ^2 is the chemical reaction parameter; Sc the Schmidt number; P_{eh} and P_{em} are the Peclet number due to heat and mass transfer, respectively; Pr the Prandtl number; Gr and Gc are the Grashof number due to temperature and concentration difference, respectively into equations (1)-(5), (6)-(9), we have

$$\frac{1}{r}\frac{\partial(ru)}{\partial r} + \frac{\psi \partial w}{\partial z} = 0 \quad (10)$$

$$\frac{\partial^2 u}{\partial r^2} + \frac{1}{r}\frac{\partial u}{\partial r} - \frac{u}{r^2} + \psi^2 \frac{\partial^2 w}{\partial z^2} = \frac{\partial p}{\partial r} + u\frac{\partial u}{\partial r} + \psi w \frac{\partial u}{\partial z} \quad (11)$$

$$\frac{\partial w}{\partial r} + \frac{1}{r}\frac{\partial w}{\partial r} + \psi^2 \frac{\partial^2 w}{\partial z^2} - \chi^2 w = \psi \frac{\partial p}{\partial z} + \psi w \frac{\partial w}{\partial z} + Gr\Theta + Gc\Phi \quad (12)$$

$$\frac{\partial^2 \Theta}{\partial r^2} + \frac{1}{r}\frac{\partial \Theta}{\partial r} + \psi^2 \frac{\partial^2 \Theta}{\partial z^2} + n^2 \Theta = Pe_h(u\frac{\partial \Theta}{\partial r} + \psi w \frac{\partial \Theta}{\partial z}) \quad (13)$$

$$\frac{\partial^2 \Phi}{\partial r^2} + \frac{1}{r}\frac{\partial \Phi}{\partial r} + \psi^2 \frac{\partial^2 \Phi}{\partial z^2} + \delta^2 \Phi = Pe_m(u\frac{\partial \Phi}{\partial r} + \psi w \frac{\partial \Phi}{\partial z}) \quad (14)$$

with the boundary conditions:

$$u = 0, w = 0, \Theta = 0, \Phi = 0 \text{ at } r = 0 \quad (15)$$

$$u = 0, \; w = 0, \Theta = \xi_1 \Theta_w, \Phi = \xi_2 \Phi_w, \; \xi_2, \xi_2 < 1 \text{ at } r = \psi \alpha z \quad (16)$$

for the upstream region and

$$u = 1, w = 1, \Theta = 1, \Phi = 1 \text{at} r = 0 \quad (17)$$

$$u = 0, w = 0, \Theta = \Theta_w, \Phi = \Phi_w \text{ at } r = 1 \quad (18)$$

for the downstream region.

With a further simplification of equations (14)-(18) on the assumptions that $\psi << 1$ such that the square of the aspect ratio becomes far too small, and the flow is fully developed such that the velocity u becomes zero on the radial axis we obtain

$$\frac{\partial w}{\partial z} = 0 \quad (19)$$

$$0 = \frac{\partial p}{\partial r} \quad (20)$$

$$\frac{\partial^2 w}{\partial r^2} + \frac{1}{r}\frac{\partial w}{\partial r} - \chi^2 w = \psi \frac{\partial p}{\partial z} + Gr\Theta + Gc\Phi \quad (21)$$

$$\frac{\partial^2 \Theta}{\partial r^2} + \frac{1}{r}\frac{\partial \Theta}{\partial r} + n^2\Theta = -Pe_h \gamma \psi w \frac{\partial \Theta}{\partial z} \quad (22)$$

$$\frac{\partial^2 \Phi}{\partial r^2} + \frac{1}{r}\frac{\partial \Phi}{\partial r} + \delta_1^2\Phi = -Pe_m \gamma \psi w \frac{\partial \Phi}{\partial z} \quad (23)$$

with the boundary conditions as stated in equations (15)-(18).

3. METHODS OF SOLUTION

Equations (21)-(23) are coupled and non-linear. For further simplification, we seek the perturbation series solutions of the form

$$s(r,z) = s^{(o)}(r,z)) + \psi s^{(1)}(r,z) + \ldots \quad (24)$$

where$\psi << 1$is the perturbation parameter. The choice of this parameter rests on the fact that it changes with the length of the channel before the merging point downstream. Therefore, it influences the Poiseuille flow structure in the region. Even so, for an additional simplification, we use $s^{(o)}(r,z) = s^{(oo)}(r) - \gamma z$ and $s^{(1)}(r,z) = s^{(10)}(r) - \gamma z$, where γ is a constant; $p(z) = Kz - \frac{K_1 z^2}{\psi}$, where$Kz$ is the pressure in the upstream, $\frac{K_1 z^2}{\psi}$ is that in the downstream, K and K_1 are constants, see [17]. Using these in equations (25)-(27) and (19)-(22), we have

The zeroth-order:

$$\frac{\partial w^{(oo)}}{\partial z} = 0 \quad (25)$$

$$\frac{\partial w^{(oo)}}{\partial r} + \frac{1}{r}\frac{\partial w^{(oo)}}{\partial r} - \chi^2 w^{(oo)} = \psi K + Gr\Theta^{(oo)} + Gc\Phi^{(oo)} \quad (26)$$

$$\frac{\partial^2 \Theta^{(oo)}}{\partial r^2} + \frac{1}{r}\frac{\partial \Theta^{(oo)}}{\partial r} + n^2\Theta^{(oo)} = 0 \quad (27)$$

$$\frac{\partial^2 \Phi^{(oo)}}{\partial r^2} + \frac{1}{r}\frac{\partial \Phi^{(oo)}}{\partial r} + \delta^2\Phi^{(oo)} = 0 \quad (28)$$

with the boundary conditions

$$w^{(oo)} = 0, \Theta^{(oo)} = 0, \Phi^{(oo)} = 0 \text{at } r = 0 \quad (29)$$

$w^{(oo)} = 0$, $\Theta^{(oo)} = \xi_1\Theta_w$,$\Phi^{(oo)} = \xi_2\Phi_w$, ξ_2 ,ξ_2<1

at $r = \psi\alpha z$ (30)

The first order:

$$\frac{\partial w^{(10)}}{\partial z} = 0 \quad (31)$$

$$\frac{\partial w^{(10)}}{\partial r} + \frac{1}{r}\frac{\partial w^{(10)}}{\partial r} - \chi^2 w^{(10)} = K_1 z + Gr\Theta^{(10)} + Gc\Phi^{(10)} \quad (32)$$

$$\frac{\partial^2 \Theta^{(10)}}{\partial r^2} + \frac{1}{r}\frac{\partial \Theta^{(10)}}{\partial r} + n^2\Theta^{(10)} = -Pe_h \gamma \psi w^{(oo)} \quad (33)$$

$$\frac{\partial^2 \Phi^{(10)}}{\partial r^2} + \frac{1}{r}\frac{\partial \Phi^{(10)}}{\partial r} + \delta^2\Phi^{(10)} = -Pe_m \gamma \psi w^{(oo)} \quad (34)$$

with the boundary conditions

$$w^{(10)} = 1, \Theta^{(10)} = 1, \Phi^{(10)} = 1 \text{ at } r = 0 \quad (35)$$

$$w^{(10)} = 0, \Theta^{(10)} = \Theta_w, \Phi^{(10)} = \Phi_w \text{ at } r = 1 \quad (36)$$

An investigation of equations (26)-(28) and (32)-(34) under the specified boundary conditions shows that they are cylindrical problems. Therefore, their solutions are of the Bessel form. In particular, the initial boundary condition $r = 0$shows that the flow starts from the origin. At this point the solutions are empty. Analytically, at this point, the Bessel function of the second kind is infinite. The constant associated with the Bessel function of the first kind is set to be unity to save the solutions from collapsing; see [22]. Solving them semi-analytically, using the Mathematica 11.2 Computational software, the solutions are still empty. It becomes necessary to shift the boundary condition $r = 0$ infinitesimally to $r = 0.001$, a point not exactly zero but highly approximately zero to obtain non-empty solutions.

4. RESULTS AND DISCUSSION

We considered the problem of merging the steady flow of sugars in the phloem vessels of a bifurcating green plant. The roles of porosity, chemical reaction, and Heat exchange parameters and merging angle on the flow are investigated, and the results are presented quantitatively and graphically. The computation was done using Mathematica 11.2 Computational software. For constant values of $\gamma = 2.0; K = 0.5; K_1 = 0.5; \xi_1 = 0.1; \xi_2 = 0.1; \Theta_w = \Phi_w = 3.0; \psi = 0.01$, Pe_h =0.2, Pe_m =0.2 and increasingly varied values of $N^2 = 0.2, 0.4, 0.6, 0.8, 1.0, 1.2$; $\alpha = 10, 15, 20, 25, 30$; $\delta^2 = 0.2, 0.4, 0.6, 0.8, 1.0, 1.2$, $\chi^2 = 0.2, 0.4, 0.6, 0.8, 1.0, 1.2$, we obtained the results shown in Fig. 2 - Fig. 7 and Table 1- Table 4.

Fig. 2 depicts that the concentration of the sugar fluid reduces with the increase in the merging angle. Additionally, the trends are oscillatory/periodic for the absolute case and sinusoidal for the real case.

More so, the concentration is seen to increase in the radially as with the increase in the radial distance. Merging angle is a function of area, and the area is a function of concentration. Therefore, the larger the area the lower the concentration. Thus, accounting for what is seen in Fig. 2.

Fig. 4 depicts that the temperature reduces as the merging angle increases and is periodic for the absolute case.

Fig. 5 depicts that an increase in the merging angle increases the sugar fluid temperature, and the structure is sinusoidal for the real case. Additionally, the temperature increases with an increase in the radial distance.

Table 1 depicts that the velocity decreases with the increases in the merging angle. However, it increases with the increase in the radial distance. An increase in the merging angle may lead to higher curvature at the merger. The flow at this point may experience a sort of whirling and rotating flow behavior.

Interactively, the combined effects of concentration and temperature levels have attendant implications on the flow velocity. The concentration, temperature, and velocity increase radially as the radial distance increases. Therefore, the decrease in the concentration and temperature have implying effects on the velocity factor in the presence of varying merging angles. The periodic and sinusoidal profiles of the concentration and temperature may lead to loss of energy for the flow.

Fig. 6 depicts that the sugar fluid temperature reduces with the increase in the heat exchange parameter (N^2). Additionally, the temperature trends depict that the energy diffusion is oscillatory/periodic. The environmental heat level depends on the radiation from the sun, and the temperature level of the plant is assumed to be lower than that of the environment. Normally, through interaction with the environment, the plant absorbs heat from the environment, and this ought to increase the plant temperature. Therefore, the decrease in the plant temperature may be due to other processes occurring in the plant.

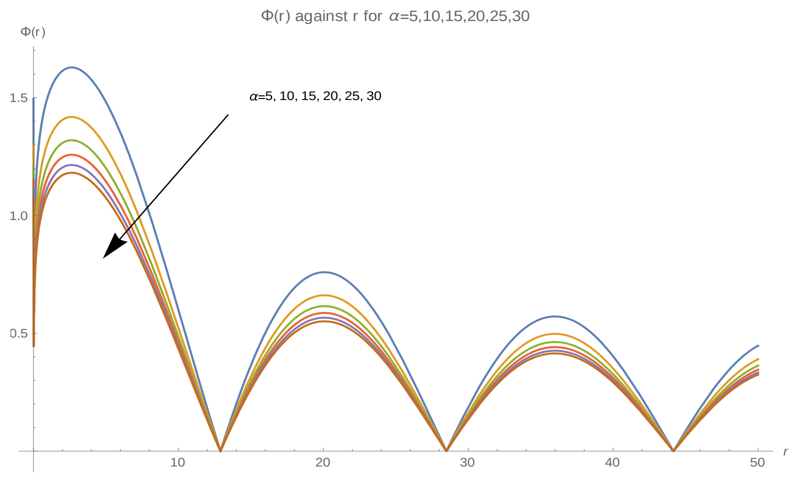

Fig. 2. Concentration - Merging angle (α) profiles for the absolute case

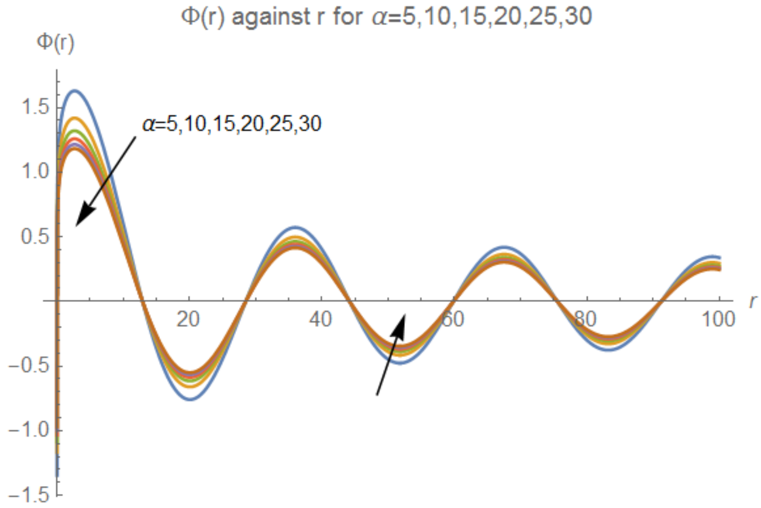

Fig. 3. Concentration - Merging angle (α) profiles for the real case

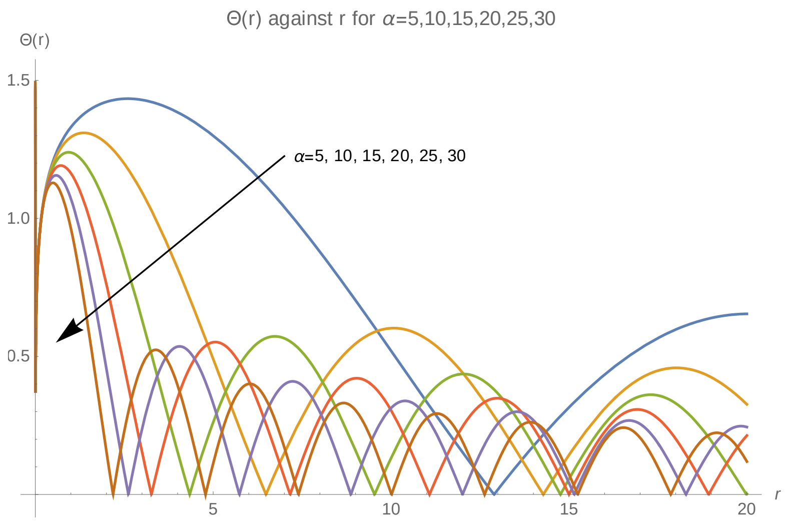

Fig. 4. Temperature-Merging angle (α) profiles for the absolute case

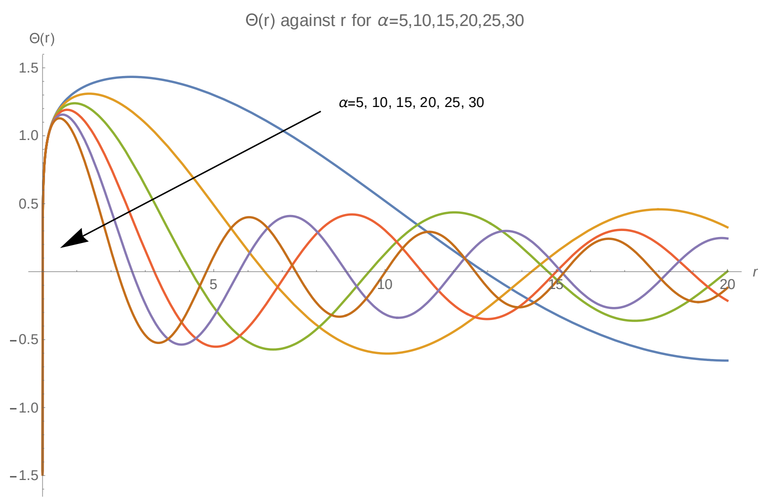

Fig. 5. Temperature-Merging angle (α) profiles for the real case

Table 1. Merging angle (α) – velocity relation

	W(α=5)	W(α=10)	W(α=15)	W(α=20)	W(α=25)	W(α=30)
W	∞	∞	∞	∞	∞	∞
0.5	23.1299	12.0696	5.5859	2.4092	0.9994	0.4049
1.0	2392.4971	1248.3922	577.7651	249.1867	103.3698	41.8790
1.5	288599.78	150589.77	69694.05	30058.64	12469.19	5051.739
2.0	3.7011×10^{7}	1.9312×10^{7}	8.9379×10^{6}	3.8549×10^{6}	1.5991×10^{6}	647859.6
2.5	4.9066×10^{9}	2.5603×10^{9}	1.1849×10^{9}	5.1104×10^{8}	2.1200×10^{8}	8.5887×10^{7}
3.0	6.6419×10^{11}	3.4657×10^{11}	1.6039×10^{11}	6.9177×10^{10}	2.8697×10^{10}	1.1626×10^{10}

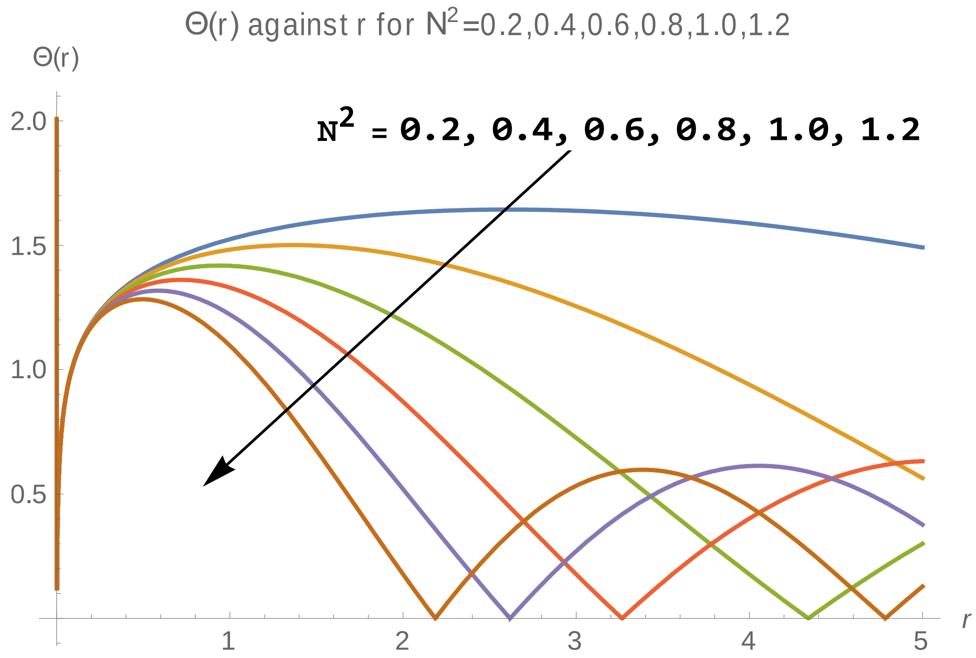

Fig. 6. Temperature-Heat ex-change (N^2) profiles for the absolute case

Table 2 depicts that the heat exchange parameter (N^2) does not affect the flow velocity of the sugar fluid. However, the velocity increases with the increase in the radial distance. Naturally, for positive heat convection existing because of the heat interaction between the plant and its environment, the velocity ought to increase. Therefore, the decreases in the velocity in the presence of variation in the heat exchange parameter could be due to other factors.

Fig. 7 depicts that the sugar fluid concentration decreases with the increase in the rate of the chemical reaction. However, it increases with the increase in the value of the radius. The trends are periodic. The mineral saltwater in the soil enters the plant through the xylem vessels. At the stomata (xylem openings) in the leaves, the water evaporates into the atmosphere. Some are retained in the mesophyll cells of matured leaves. This water reacts with the carbon dioxide from the atmosphere which diffuses into the matured leaves. This reaction, in the presence of sunlight (as the activation energy), produces synthesized sugar/carbohydrate through the process of photosynthesis. The sugars are translocated through the phloem vessels to other parts of the plant, where they are used for metabolism and growth or stored. The decreases in the concentration due to an increase in the rate of chemical reaction has implying effects on the flow velocity, concentration is a function of velocity. Similarly, the decrease in the concentration implies that the rate of interaction of the fluid particles, which affects the flow velocity is reduced.

Table 2. Heat ex-change (N^2)–Velocity relation

	W(N=$\sqrt{0.1}$)	W(N=$\sqrt{0.3}$)	W(N=$\sqrt{0.5}$)	W(N=$\sqrt{0.7}$)	W(N=$\sqrt{0.9}$)	W(N=$\sqrt{1.2}$)
W	Indeterminate	Indeterminate	Indeterminate	Indeterminate	Indeterminate	Indeterminate
0.5	12.1827	12.408	12.8792	13.642	14.7791	17.5291
1.0	131052.	133476.	138545.	146751.	158983.	188565.
1.5	1.8625×10^{9}	1.8969×10^{9}	1.9689×10^{9}	2.0856×10^{9}	2.2594×10^{9}	2.6798×10^{9}
2.0	3.0318×10^{13}	3.0878×10^{13}	3.2051×10^{13}	3.3949×10^{13}	3.6779×10^{13}	4.3623×10^{13}
2.5	5.2974×10^{17}	5.3953×10^{17}	5.6002×10^{17}	5.9319×10^{17}	6.4264×10^{17}	7.6221×10^{17}
3.0	9.6359×10^{21}	9.8141×10^{21}	1.0187×10^{22}	1.0790×10^{22}	1.1690×10^{22}	1.3865×10^{22}

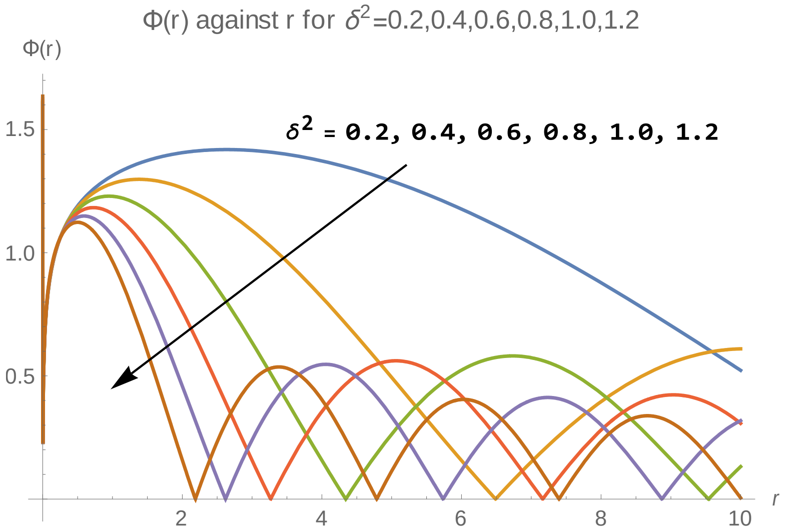

Fig. 7. Concentration-chemical reaction (δ^2) profiles

Table 3. Velocity-Chemical Reaction relation

	W($\delta = \sqrt{0.2}$)	W($\delta = \sqrt{0.4}$)	W($\delta = \sqrt{0.6}$)	W($\delta = \sqrt{0.8}$)	W($\delta = \sqrt{1.0}$)	W($\delta = \sqrt{1.2}$)
W	Indeterminate	Indeterminate	Indeterminate	Indeterminate	Indeterminate	Indeterminate
0.5	6.6191	6.8203	7.1777	7.7285	8.5382	9.7222
1.0	3265.2	3364.91	3541.69	3814.05	4214.43	4799.83
1.5	4.7415×10^{7}	4.8863×10^{7}	5.1430×10^{7}	5.5385×10^{7}	6.1199×10^{7}	6.9699×10^{7}
2.0	7.72104×10^{11}	7.9568×10^{11}	8.3749×10^{11}	9.0189×10^{11}	9.9656×10^{11}	1.1350×10^{12}
2.5	1.3491×10^{16}	1.3903×10^{16}	1.4633×10^{16}	1.5759×10^{16}	1.7413×10^{16}	1.9832×10^{16}
3.0	2.454×10^{20}	2.5289×10^{20}	2.6618×10^{20}	2.8665×10^{20}	3.1674×10^{20}	3.6074×10^{20}

Table 4. Velocity-porosity relation

	W($\chi = \sqrt{0.2}$)	W($\chi = \sqrt{0.4}$)	W($\chi = \sqrt{0.6}$)	W($\chi = \sqrt{0.8}$)	W($\chi = \sqrt{1.0}$)	W($\chi = \sqrt{1.2}$)
W	∞	∞	∞	∞	∞	∞
0.5	0.2092	0.1249	0.0873	0.0661	0.0531	0.0453
1.0	0.3895	0.2611	0.2211	0.2125	0.2209	0.2417
1.5	0.5909	0.4397	0.4236	0.4652	0.5534	0.6955
2.0	0.7991	0.6570	0.7167	0.9025	1.2440	1.8301
2.5	1.0166	0.9293	1.1583	1.6941	2.7474	4.8070
3.0	1.2484	1.2800	1.8425	3.1675	6.1186	12.8804

Table 3 shows that the velocity increases with the increase in the rate of the chemical reaction. More so, it increases with the increase in radial distance. As the rate of chemical reaction increases, the interaction of the fluid particles increases, and this leads to an increase in the flow velocity.

Table 4 shows that increase in the porosity parameter produces fluctuation in the flow velocity structure. At some points, it decreases and at some other points, it rises as the porosity parameter increases. However, the velocity increases as the radius increases.

5. CONCLUSION

The transport of synthesized sugar fluid in the phloem vessels of a green plant to points where they are used for metabolism or stored through a merger is examined. The analysis of results shows that the increase in:

- Conflux angle reduces the concentration, temperature, and velocity of the fluid, and with fluctuations in the concentration and temperature structures.
- The heat exchange parameter reduces the fluid temperature but does not affect the flow velocity.
- The rate of chemical reaction decreases the concentration but enhances the flow velocity.
- The porosity of the vessels reduces the flow velocity.

ACKNOWLEDGEMENT

The equations used in this work were culled from Okuyade and Abbey (2017) under the Creative Common Attribution License

COMPETING INTERESTS

Authors have declared that no competing interests exist.

REFERENCES

1. Herve Cochard, The basics of plants hydraulics, Journal of Hydraulics. 2013;1:e-00001.
2. Jensen KH, Berg-Sorensen H, Bruus NM, Holbrook J, Liesch A, Schulz MA, Zwienniecki, Bohr T. Sap flow and sugar transportation in plants, Review of Modern Physics. 2016;88:1-63.
3. Knoblauch M, van Bel AJE. Sieve tubes in action. Plant Cell. 1998;10:35–50.
4. Badre H, Dennis SCR, Smith FT. Numerical and asymptotic solutions for merging flow through a channel with an upstream splitter plate. Journal of Fluid Mechanics. 1985;156:63-81.
5. Krijger JK, Hillen B. Steady two-dimensional merging flow from two channels into a single channel. Applied Scientific Research. 1990;47(3):233-246.
6. Siddiqui AA. Numerical simulation of asymmetric merging flow in a rectangular channel. World Journal of Mechanics. 2016;6:118-130. Available:http://dx.doi.org/10.4236/wjm.2016.64010
7. Niklas KJ. Plant allometry: The scaling of plant form and process. University of Chicago Press, Chicago; 1994.
8. Nobel PS. Physicochemical and environmental plant physiology. Academic Press, Boston; 2009.
9. Taiz L, Zeiger E. Plant physiology. 5th ed. Sinauer Associates, Inc., Sunderland, MA; 2010.
10. Morris JR, Hartl DL, Knoll AH, Lue RA, Berry A, Biewener A, et al. Biology: How life works. 1st ed. W. H. Freeman, New York, NY; 2013.
11. Voge S. Comparative Biomechanics: Life’s physical world. 2nd ed. Princeton University Press, Princeton, NJ; 2013.
12. Rand RH. Fluid mechanics of green plants, Annu. Rev. Fluid Mech. 1983;1:29–45.
13. Gibson LJ. The hierarchical structure and mechanics of plant materials, J. R. Soc. Interface. 2012;9.
14. Dumais J, Forterre Y. Vegetable dynamicks: The role of water in plant movements, Annu. Rev. Fluid Mech. 2012;44:453–478.
15. De Schepper V, De Swaef T, Bauweraerts I, Steppe K. Phloem transport: A review of mechanisms and controls, J. Exp.Bot. 2013 64:4839–4850.
16. Stroock AD, Pagay VV, Zwieniecki MA, Holbrook NM. The physicochemical; 2014.
17. Okuyade WIA, Abbey TM. Steady oscillatory flow in a bifurcating green plant, Asian Research Journal of Mathematics, ScienceDomain International. 2017;2(4):1-19. DOI: 10.9734/ARJOM/2017/31306.

18. Okuyade WIA, Abbey TM. Biomechanics of a bifurcating green plant-Part 1, Asian Journal of Physical Sciences, ScienceDomain International. 2017;1(2):1-22.
DOI: 10.9734/AJOPS/2017/31458.
19. Okuyade WIA, Abbey TM. Biomechanics of a bifurcating green plant- Part 2: Thermal environmental effect, Asian Journal of Physical and Chemical Sciences, ScienceDomain International. 2017;2(3):1-14.
DOI: 10.9734/AJOPS/2016/31458.
20. Bestman AR. Global models for the biomechanics of green plants, part 1. International Journal of Energy Research. 1991;19:677– 684.
21. Tadjfar M, Smith FT, Direct simulation and modeling of basic 3-dimensional bifurcating tube flow, Journal Fluid Mechanics. 2004;519:1-32.
22. Erwin Kreyzig. Advanced engineering mathematics, John Wiley and Sons, Incorporation, New Delhi, India; 1983.

Peer-review history:
The peer review history for this paper can be accessed here:
http://www.sdiarticle4.com/review-history/66992